



Since January 2020 Elsevier has created a COVID-19 resource centre with free information in English and Mandarin on the novel coronavirus COVID-19. The COVID-19 resource centre is hosted on Elsevier Connect, the company's public news and information website.

Elsevier hereby grants permission to make all its COVID-19-related research that is available on the COVID-19 resource centre - including this research content - immediately available in PubMed Central and other publicly funded repositories, such as the WHO COVID database with rights for unrestricted research re-use and analyses in any form or by any means with acknowledgement of the original source. These permissions are granted for free by Elsevier for as long as the COVID-19 resource centre remains active.



## Research paper

# Castanospermine reduces Zika virus infection-associated seizure by inhibiting both the viral load and inflammation in mouse models

Anil M. Tharappel<sup>a,\*\*</sup>, Yichen Cheng<sup>a</sup>, Eric H. Holmes<sup>b</sup>, Gary K. Ostrander<sup>b</sup>, Hengli Tang<sup>a,\*</sup>

<sup>a</sup> Department of Biological Science, Florida State University, 319 Stadium Dr., Tallahassee, FL, 32306-4295, USA

<sup>b</sup> Department of Biomedical Sciences, College of Medicine, Florida State University, 319 Stadium Drive, Tallahassee, FL, 32306, USA

## ARTICLE INFO

## Keywords:

Zika virus  
Castanospermine  
Seizure  
Inflammation

## ABSTRACT

Zika virus (ZIKV) outbreaks have been reported worldwide, including a recent occurrence in Brazil where it spread rapidly, and an association with increased cases of microcephaly was observed in addition to neurological issues such as GBS that were reported during previous outbreaks. Following infection of neuronal tissues, ZIKV can cause inflammation, which may lead to neuronal abnormalities, including seizures and paralysis. Therefore, a drug containing both anti-viral and immunosuppressive properties would be of great importance in combating ZIKV related neurological abnormalities. Castanospermine (CST) is potentially a right candidate drug as it reduced viral load and brain inflammation with the resulting appearance of delayed neuronal disorders, including seizures and paralysis in an *Ifnar1*<sup>-/-</sup> mouse.

## 1. Introduction

Since its discovery in 1947 in Uganda, the Zika virus (ZIKV) has spread throughout the world, causing significant outbreaks in Micronesia in 2007, French Polynesia in 2013, and Brazil in 2015. The spread of the virus to North America began in 2016 and was coincident with the World Health Organization declaring ZIKV a Public Health Emergency. Although the incidence of ZIKV infection has declined in recent years, the chances of another outbreak cannot be ruled out. Several vaccines and small molecules are in preclinical or clinical trials, but presently, there is no approved drug on the market for the treatment of ZIKV. Additionally, since antibody-mediated enhancement is reported with the closely related dengue virus DENV (Dejnirattisai et al., 2016), the vaccine against the ZIKV may take longer to reach the market.

ZIKV is a positive-sense, single-stranded RNA virus that belongs to the flaviviridae family, flavivirus genus, and transmitted by *Aedes* mosquitos. The genome is ~11,000 nt that encodes three structural proteins, including capsid (C), precursor membrane (prM), and envelope (E) as well as seven non-structural proteins (NS1, NS2A, NS2B, NS3, NS4A, NS4B, and NS5). Of these proteins, NS1, E and prM are glycosylated. The glycosylation of flaviviral NS1 appears to be essential for efficient secretion, virulence and viral replication (Annamalai et al., 2019; Crabtree et al., 2005; Pryor and Wright, 1994; Somnuk et al.,

2011; Winkler et al., 1988). The ZIKV E protein is glycosylated at amino acid N154. In mouse models, recombinant N154Q ZIKV that lacks the E protein glycosylation results in lower viremia, decreased weight loss, and no mortality although it does not significantly affect neurovirulence (Fontes-Garfias et al., 2017). The prM of flaviviruses facilitates the folding and trafficking of the E protein at the time of virus particle biogenesis (Allison et al., 1995; Heinz et al., 1994). The cellular protease furin cleaves prM during particle egress, releasing an N-terminal fragment (pr) containing the single N-linked glycan of prM. This cleavage is required for infectivity in flaviviruses (Elshuber et al., 2003).

Only 20% of ZIKV infections are symptomatic, characterized by low-grade fever, pruritic maculopapular rash, myalgia, arthralgia, conjunctivitis, and headache. Although ZIKV symptoms are less severe than the closely related dengue virus (DENV), neurological abnormalities such as microcephaly in infants (Mlakar et al., 2016; Moura da Silva et al., 2016), Gullian Barre syndrome (GBS) in adults (Brasil et al., 2016; Cao-Lormeau et al., 2016; Kassavetis et al., 2016; Rozé et al., 2017), and the possibility of sexual transmission (Petridou et al., 2019; Reyes et al., 2019) makes the ZIKV disease more complicated and of high concern. Among 35 ZIKV-infected infants with microcephaly in Brazil, other neurological abnormalities reported included hypertonia/spasticity (37%) and seizure (9%). Of the 27 available neuroimages from these infants, all presented with wide-spread brain calcification and evidence of cell migration abnormalities (Schuler-Faccini et al., 2016).

\* Corresponding author.

\*\* Corresponding author.

E-mail address: [tang@bio.fsu.edu](mailto:tang@bio.fsu.edu) (H. Tang).

**Abbreviations**

ZIKV	Zika virus
MOI	multiplicity of infection
Dpi	days of post-infection
CST	castanospermine
Ffu	focus forming unit
FFA	focus forming assay
IP	intraperitoneally
C	capsid protein
E	envelope protein
GBS	Guillain Barré syndrome

GFAP	glial fibrillary acidic protein
TMEV	Theiler's murine encephalomyelitis virus
EEG	electroencephalogram
ER	endoplasmic reticulum
HIV	human immunodeficiency virus
FBS	fetal bovine serum
BDVD	bovine viral diarrhea virus
DMEM	Dulbecco's modified Eagle's medium
RPMI	Roswell Park memorial institute medium
ATCC	American type culture collection
HRP	horseradish peroxidase
Bw	body weight

Encephalopathy and seizures were reported in a patient with ZIKV infection (Asadi-Pooya, 2016; Pastula et al., 2016; Rozé et al., 2016). Finally, motor abnormalities and epilepsy were reported in children with congenital ZIKV infection (Pessoa et al., 2018).

Seizure-related activities have also been reported in various animal models with ZIKV infection. Neonatal mice with blocked interferon signalling have been used in ZIKV viral infection studies. In addition to lethal infection, these mice also displayed neurological symptoms such as toe walking, tremors, loss of balance, paralysis and hunched posture (Aliota et al., 2016; Lazear et al., 2016; Manangeeswaran et al., 2016; Rossi et al., 2016). The seizure-related activity was seen in a ZIKV infected immunocompetent neonatal mouse (Manangeeswaran et al., 2016). In adult AG129 mice, the seizures were independent of hind limb motor deficit levels (Zukor et al., 2018). The seizure-related activity has been reported in piglets with in-utero exposure to ZIKV (Darbellay et al., 2017). In a nonhuman primate model (*Macaca mulatta*), the infants displayed a range of neurodevelopmental phenotypes and pathologies, from seizure activity and motor delay (Steinbach et al., 2020).

It is well known that brain inflammation can cause seizures. ZIKV infection can cause myelitis and encephalitis in AG129 adult mice (Zukor et al., 2018). Astrocytes play an important role in brain inflammation. With ZIKV infection, there was an increase in the expression of glial fibrillary acidic protein (GFAP) a marker of astrocytes (Souza et al., 2018). ZIKV infection is associated with inflammation and synaptic retractions in motor neurons (Morrey et al., 2019; Zukor et al., 2018). The motor abnormalities can be assessed by rotarod and wire suspension tests (Barker-Haliski et al., 2016; Rabl et al., 2016).

Repurposing approved or lead molecules will cut down the delay in the development of drugs for ZIKV. Several anti-viral candidates are directed to viral structural proteins and enzymes (Li et al., 2019; Shiryaev et al., 2017) have been identified. There is vast potential for the drugs which interfere with host factors involved in ZIKV life cycle, starting from attachment to post-translational modification (Saiz et al., 2018). Iminosugars are glucose mimetics with a nitrogen atom in place of ring oxygen (Dwek et al., 2002). Some of the iminosugars are known to have anti-viral activity in human immunodeficiency virus (HIV) (Taylor et al., 1994), pestivirus-bovine viral diarrhea virus (BVDV) (Whitby et al., 2004), dengue virus (DENV) (Sayce et al., 2016) and filovirus (Warfield et al., 2017). They inhibit alpha-glucosidase enzyme present in endoplasmic reticulum (ER), thus hindering the glycation of the viral particles. Several viruses have glycosylated structural as well as non-structural proteins. N-linked glycosylation is the most common type of glycosylation process, that occurs in the ER lumen in eukaryotes (Chang et al., 2013a). The folding of the glycoproteins of many enveloped viruses is far more dependent upon the calnexin pathway of protein folding than are most host glycoproteins, and drugs that inhibit this pathway would be expected to be selectively anti-viral (Chang et al., 2013b). C-type lectins recognize carbohydrate structures present on viral glycoproteins and function as attachment factors for several enveloped viruses. Changes in the glycan structures associated with viral

glycoproteins may also alter their interaction with C-type lectins and consequently inhibit pro-inflammatory cytokine production (Perry et al., 2013).

Castanospermine (CST) is an octahydroindolizine alkaloid that was first isolated from the seeds of the brown bean tree *Castanospermum australe* (Hohenschutz et al., 1981). Multiple activities of CST have been reported including inhibition of the ER glucosidase inhibitors I and II and thus interfering with oligosaccharide post-translational processing (Caputo et al., 2016; Elbein, 1991). CST also exhibits anti-inflammatory activity in transplant rejection (Bartlett et al., 1994; den Dulk et al., 2004), autoimmune encephalomyelitis and adjuvant arthritis (Walter et al., 2002; Willenborg et al., 1992, 1989). The potency of CST varies with cell type and the virus. CST exhibited an IC<sub>50</sub> of 87 µM towards DENV2 in human hepatoma cells (Huh-7) and 1 µM in baby hamster kidney cells (Whitby et al., 2005). CST inhibits BVDV with IC<sub>50</sub> 110 µM and 567 µM in plaque inhibition assay and cytopathic effect assay, respectively in Madin-Darby bovine kidney (MDBK) cells (Whitby et al., 2004). The activity of CST against HIV has also been reported (Sunkara et al., 1990; Taylor et al., 1994; Walker et al., 1987). The weak activity in cellular assays is possibly due to its highly polar nature (Shi et al., 2011). Celgosivir (6-O-butanoyl castanospermine) is a pro-drug that is immediately converted to CST by esterase. Celgosivir is found to have better cell permeability, activity against glucosidase-I and anti-viral potency. In clinical studies among patients with secondary DENV infection, a small, non-statistical trend towards better outcome on platelet nadir and the difference between the maximum and minimum hematocrit was observed in celgosivir-treated patients (Sung et al., 2016). Herein we evaluated CST impact on another member of the flavivirus family, as we examined the anti-ZIKV activity of CST *in vivo* both in pre- and post-infection treatments in a murine model. In addition to antiviral activity, we also evaluated CST for its efficacy against ZIKV induced neurological abnormalities such as seizure, paralysis and motor function.

## 2. Material and methods

### 2.1. Cell culture, virus strains, and reagents

Vero E6 cells were maintained in Dulbecco's modified Eagle's medium (DMEM, HyClone) supplemented with 10% fetal bovine serum (FBS, Sigma-Aldrich). SNB-19, human glioblastoma cells were maintained in RPMI-1640 medium (ATCC) with 10% FBS. Zika virus strains used were: FSS13025 (Cambodia, 2010), ZIKV PRVABC59 (Puerto Rico, 2015), and ZIKV MR766 (Uganda, 1947). ZIKV stocks were prepared by infecting *Aedes albopictus* (C6/36) cells at multiplicity of infection (MOI) of 0.1 and were incubated with the viral inoculum for 1 h at room temperature. Fresh medium was added to the culture flask and incubated at 28 °C till 8–10 days. The supernatant was collected and filtered through 0.45 µm, and frozen in aliquots at –80 °C. Virus stock was tittered in Vero E6 cells before infecting with mice and SNB-19 cells.

## 2.2. Extraction and purification of castanospermine

Castanospermine (1,6,7,8-tetrahydroxyoctahydroindolizine) was isolated from the seeds of the Australian legume *C. australe* as per previously published protocol (Hohenschutz et al., 1981). Briefly, finely ground immature seed (3 kg) of *C. australe* was extracted with 75% ethanol (3 × 3 L). After filtration, the extract was mixed with strongly acidic cation exchange resin (Dowex-50) in the H<sup>+</sup> form and stirred overnight. After stirring, the resin was allowed to settle, and the liquid was poured off. The resin was batch washed extensively with deionized water until the washings were clear and the resin then poured into a column. The column was eluted with 2 M NH<sub>4</sub>OH and the eluate fractions were concentrated by rotary evaporation until all ammonia was removed. The concentrated eluate was then loaded onto a column of Dowex-50, pyridinium ion form, washed extensively with deionized water and eluted first with 2 M pyridine followed by 2 M NH<sub>4</sub>OH. Fractions containing CST were pooled, concentrated to near dryness, and crystallized in 95% ethanol. The white crystals were filtered, air dried, and used in these experiments. The purity and identity of the CST were determined by LC/MS and NMR analysis, respectively.

## 2.3. Viral titre by focus-forming assay (FFA)

Human glioblastoma-derived cells (SNB-19), were seeded in 96-well plates in RPMI-1640 medium containing 10% FBS, 100 units/ml penicillin and 50 µg/mL streptomycin. The cells were incubated at 37 °C in CO<sub>2</sub> incubator and grown to ~80% confluence. The media was replaced with fresh media containing either CST (0.3–3000 µM, 3 fold dilutions) or phosphate buffer saline (PBS) as vehicle control. After 1 h of pre-treatment, cells were infected with ZIKV at a MOI of 1. The plates were incubated at 37 °C in a 5% CO<sub>2</sub> incubator for 24 h. Cell supernatant was titrated in duplicates onto a monolayer culture of Vero E6 cells in 96-well plates with log dilution and incubated at 37 °C for 2 h in CO<sub>2</sub> incubator. Virus inoculum was removed and replaced with RPMI medium with 1% methylcellulose overlay. Vero cells were incubated for an additional 48 h, removed the overlay before fixation with 4% formaldehyde, blocked and incubation with anti-flavivirus group antibody (4G2) overnight at 4 °C. Cells were washed three times with PBS and incubated with horseradish peroxidase (HRP)-conjugated anti-mouse secondary antibody for 1 h at room temperature. Plates were washed with PBS and incubated with DAB peroxidase substrate (SK4100, Vector Labs) for 10 min, and the reaction stopped by washing with water. Focus forming units (ffu) were counted by the naked eye and confirmed by counting by 40x microscopy. The IC<sub>50</sub> was calculated using Graphpad prism software version 8.

## 2.4. Cell toxicity assay

The tolerance level of CST to SNB19 was indirectly estimated by measuring the adenosine triphosphate (ATP) content of the SNB19 cells treated with various concentrations of the CST using CellTiter Glo reagent (G7571, Promega). Cells were seeded in opaque walled 96-well plates in RPMI-1640 medium 10% FBS, 100 units/ml penicillin and 50 µg/ml streptomycin, incubated at 37 °C with 5% CO<sub>2</sub> until the cells reached ~80% confluency. Media was then replaced with fresh media containing CST (0.001–300 mM) or PBS as vehicle control. After incubating the cells for 24 h at 37 °C in CO<sub>2</sub> incubator, 100 µl of CellTiter Glo reagent was added. The luminescence was recorded using luminometer (9300–001, Turner Biosystems). The 50% cytotoxic concentration (CC<sub>50</sub>) was calculated using Graphpad prism software version 8.

## 2.5. Western blot analysis

SNB19 cells were grown in 6-well-plates in RPMI-1640 medium 10% FBS, 100 units/ml penicillin and 50 µg/mL streptomycin, to 80% confluence and treated with or without CST (100, 500 and 1000 µM) for

24 h. Cells were harvested by trypsinization, pelleted, lysed in 1X Laemmli buffer, and the lysates boiled. The lysates were run on SDS-PAGE, and separated protein bands were transferred to nitrocellulose membrane followed by blocking with 5% powdered skimmed milk in PBS with 0.1% Tween 20. Primary antibody anti-ZIKV NS1 (BF-1225-36, BioFront Technologies, Tallahassee, FL) was added and incubated for overnight at 4 °C. The reaction was visualized with HRP-linked anti-mouse secondary antibody followed by enhanced chemiluminescence (WBKLS0500 Millipore). For loading control, anti-GAPDH (sc-25778, Santa Cruz Biotechnology, Texas) was used as a primary antibody.

## 2.6. Mouse studies

All the studies were completed with adult (6–8 wk old) *ifnar1*<sup>-/-</sup> mice which were of C57 background (Jackson lab). Upon arrival mice were quarantined for a week, fed ad libitum, provided 12 h dark/12 h light cycle. The mouse-adapted ZIKV FSS13025 strain was used for all the mouse studies. The virus and drug were dosed intraperitoneally (IP). Stocks of the virus stored at –80 °C was diluted in serum-free EMEM media as required for each study. The CST was dissolved in physiological saline such that 100 µl will have required dose per mouse as indicated in individual studies. Five *in vivo* studies were conducted, and treatment groups in each study were compared by statistical analysis using unpaired Student's *t*-test using Graphpad prism version 8.

### 2.6.1. Mouse-study-I: single dose of CST per day to check viral load

*ifnar1*<sup>-/-</sup> mice (6 to 7-wk old, male and female) were dosed with CST (IP, 50 mg/kg or 100 mg/kg bw) or vehicle control (0.9% saline) once daily on day 0 to day 3 for a total 4 doses. Mice were infected with ZIKV (10<sup>4</sup> ffu/in 100 µl EMEM media/mouse IP) on day 0. Mice were euthanized on day 3 dpi. Blood and liver tissue were collected, serum was separated from the blood and the NS1 antigen level in the serum was estimated by an enzyme linked immunosorbent assay (ELISA) kit (BioFront Technologies, Tallahassee, FL) as described in the manual. Liver tissue was stored in RNA-later (Qiagen) at 4 °C, around 30 mg of the tissue was homogenised in 600 µl of buffer RLT (79,216, Qiagen) with 10 µl/ml beta mercaptoethanol using Tissue Ruptor II (Qiagen). After centrifuging at 14,000 g, the supernatant was transferred to a new tube and added I volume of 70% ethanol. After mixing, 700 µl of the solution is loaded on to QIAamp Mini Spin Columns and RNA was extracted using the QIAamp viral RNA mini kit (52,904, Qiagen). RNA (2 µg) was converted to cDNA using Superscript III First strand synthesis (Invitrogen), and expression levels of ZIKV-NS1 gene relative to mouse GAPDH gene was done using the specific primers (Supplementary Table 1) by real time PCR.

### 2.6.2. Mouse-study-II: single dose of CST per day to study the survivability

*ifnar1*<sup>-/-</sup> mice (6 to 7-wk-old, male and female) were randomly grouped into 4 groups with equal number of males and females in each group. G1: CST 200 mg/kg & media, G2: virus & saline, G3: virus & CST 100 mg/kg, G4: virus & CST 200 mg/kg. Mice were treated with CST (100 mg or 200 mg/kg bw) or saline once daily until seven doses starting from day 0 were given. Mice were infected with ZIKV (10<sup>4</sup> ffu/mouse, IP) on day 0 in 100 µl EMEM media. Two to six mice were euthanized from each group on day 3 to estimate systemic and tissue viral load. The remaining mice were observed for death/morbidity until day 10. End-points were decided based on the published articles (Dowall et al., 2016; Morton, 2000; Olfert and Godson, 2000) and our previous studies (Yang et al., 2018). Mice reaching endpoints (Table 1) were euthanized as per the approved protocol. Based on the previous study, the mice which reached endpoints before day 5 dpi were not considered for statistical analysis as death due to viral infection happens on or after day 5 dpi. The statistical analysis was done using Kaplan Meier equation and comparison of survival curves was done using log rank (Matnel-Cox) test.

**Table 1**  
Scoring and end point criteria for mice survivability study.

Posture	(Normal = 0; slightly hunched = 1; moderately hunched = 2; severally hunched = 3)
Coat condition	(Normal/groomed = 0; rough = 1; ruffled/unkept = 2)
Activity/ Alertness	(Normal = 0; reduced exploratory activity = 1; slow moving, dull or depressed = 2; not moving = 3)
Movement/Gait	(Normal = 0; slight incoordination/decreased righting response = 1; tiptoe walking or altered gait involving 1 limb = 2; staggering or paralysis or tremors of 2 or more limbs = 3)

End points.

- Body weight loss is equal to or greater than 20% of baseline.
- One limb paralyzed and body weight loss equal to or greater than 15% of baseline.
- Both limbs paralyzed and body weight loss equal to or greater than 12% of baseline.
- Assessment score of 3 for any of the following clinical observations: Activity/Alertness or Movement/Gait.
- A total assessment score of 6 plus 10% body weight loss.
- Found dead.

**2.6.3. Mouse-study-III: split doses of CST to study survivability**

In this study, the mice were dosed with 100 mg/kg CST twice a day 24 h before (preCST) or 24 h after (posCST) infection with lesser ZIKV load ( $10^3$  ffu/mouse). Six to seven-week-old *ifnar1<sup>-/-</sup>* (male and female) mice were grouped. G1: Saline and EMEM ( $n = 2$ ), G2: preCST-100X2 + EMEM media ( $n = 1$ ), G3: posCST-100X2 + EMEM media ( $n = 1$ ), G4: ZIKV + Saline ( $n = 8$ ), G5: ZIKV + preCST ( $n = 8$ ), G6: ZIKV + posCST ( $n = 8$ ). A survival blood sampling was done from the tail on day 3 for estimating the NS1 antigen by ELISA as a measure of viral load. The treatment was continued until day 6 dpi and scored as described in mouse-study-II above. Remaining mice were observed for morbidity/death until day 10. Mice reaching end points (Table 1) were euthanized and on day 10, all the remaining mice were euthanized. Seizure-related activity and hind limb paralysis were also noted. Statistical analysis was done with the Kaplan Meier equation and comparison of survival curves was done using log-rank (Matnel-Cox) test.

**2.6.4. Mouse-study-IV: ZIKV induced inflammation of the brain and treatment with CST**

The study design follows mouse-study-III but was terminated at day 4 dpi. Survival blood sampling was conducted daily from day 2 to day 4 dpi from the tail vein to estimate viral load using the ZIKV-NS1 ELISA kit. Following euthanization on day 4 dpi, brain tissues were collected in Trizol, snap-frozen and stored at  $-70$  °C. RNA was isolated, converted to cDNA and the relative expression of genes of ZIKV- NS1 and inflammation associated genes (IL1- $\beta$ , TNFa, IL6, IL10, GFAP, iNOS1) were determined using real time PCR. Mouse glyceraldehyde 3-phosphate dehydrogenase (GAPDH) was used as a house-keeping gene. The estimation ZIKV RNA copy number from blood collected on day 4 dpi is explained separately in detail. The primers used were listed in the [Supplementary Table1](#).

**2.6.5. Mouse-study-V: effect of CST on provoked seizure and other neuronal abnormalities**

We tested the effect of CST on seizure-related activities following ZIKV infection and the study continued until day 10. *ifnar1<sup>-/-</sup>* mice (6–7 wk old, male and female) were treated and infected as described in mouse-study-III except the viral load which was  $2 \times 10^3$  ffu/mouse. On day (–1), day 3, day 5, day 6 and day 7 dpi, the mice were observed for provoked as well as spontaneous seizures. Hind limb paralysis was assessed by open-field testing and the motor co-ordination by rotarod testing.

**2.6.5.1. Inverted grid suspension test.** Inverted grid suspension test was done as based on the published protocol (Deacon, 2013) in mouse-study-V on day (–1), day 3, day 5 and day 6. A rectangular screen

made of stainless steel ( $18 \times 12$  inch) with  $1 \text{ cm}^2$  mesh was used. The side of the screen was covered with sealing tape to prevent mice climbing to the top of the mesh. For testing, the mouse was placed in the centre of the wire mesh screen; a timer was started, and the screen was rotated to an inverted position over 2 s with the mouse's head declining first. The screen was held steady 40 cm above a padded surface. Time was noted when the mouse fell off or was removed when the criterion time of 120 s was reached (Rabl et al., 2016). Each mouse was trained two times before the actual reading was taken. Video recording was done using a handycam (Sony) mounted on a stand.

**2.6.5.2. Paralysis test.** The test was done during mouse-study-V on day (–1), day 3, day 5, day 6 and day 7. Each mouse was held on its tail and lifted to a height of 30 cm, and movements of the limbs were noted, and video recorded. Further, the mouse was allowed to walk on a mounted flat surface and observed for paralysis or any other walking disabilities. Video recording was done using a handycam (Sony) mounted on a stand.

**2.6.5.3. Provoked seizure test.** The test was done during mouse-study-V on day (–1), day 3, day 5, day 6 and day 7. The provoked (acute symptomatic) seizure test was conducted based on the observation in previous studies that there is a seizure-related activity in mice during the opening of the cage lid or handling of mice, especially in the morning. Hence, we decided to observe the mice for seizure and related activity in the morning from 9 to 11 a.m. The mouse cages were brought to the hood between 9 and 10 a.m., and the camera was focussed on the cage for video recording. To induce uniform handling stress, mice were picked up by the tail and lifted to a height of 10 inches and dropped to the cage bedding three times. Seizure and related activity, if any, was noted and scored (Racine, 1972) along with the addition of other symptoms such as toe walking, hunched position, erratic running and jumping upon touching as indicated in Table 2. (Lüttjohann et al., 2009). Mice with a Racine score of at least one (Score 5 and above in Table 2) were considered as exhibiting a seizure. Some of the mice exhibited the seizure and related activity while opening the cage lid while others showed this activity after dropping to the cage bed.

**2.6.5.4. Measure of spontaneous seizure and related activity.** During mouse-study-V, the mice in their cages were observed randomly for any seizure, and related activity between 8 a.m. and 7 p.m. On day 6 of pdi, 1 h video recording of the mice in their cages were done using a handycam mounted on a stand.

**2.6.5.5. Rotarod test.** During the mouse-study-V, rotarod testing was done using rotarod test equipment (Panlab, 76–0770, rod dia 1 inch, fall height 20 cm) as per published protocol (Rabl et al., 2016). The mice were habituated to the testing system before stating the study until they were able to stay on the rotating rod for at least 1 min at a constant speed of 4 rpm. Mice were trained 2–3 times before conducting the actual test. Each mouse was lifted from the cage by their tail and placed on the rod, and the rod was rotated with an initial speed of 4 rpm until the mouse stabilized itself, and then the speed was accelerating up to 40 rpm. The mice falling before 5 s were not considered in the analysis. The trial

**Table 2**  
Seizure scoring sheet (RS: Racine stages).

Sl. No	Neurological Abnormalities	Score
1	Toe walking	1
2	Hunched dorsal position	2
3	Erratic running	3
4	Jumping upon touching	4
5	Mouth and facial movement (RS-1)	5
6	Head nodding (RS-2)	6
7	Forelimb clonus (RS-3)	7
8	Rearing with forelimb clonus (RS-4)	8
9	Rearing and falling with forelimb clonus (RS-5)	9

began when acceleration was started and ended when the animal fall-off the rod. If the animal clung to the rod and completed the full passive rotation, the timer was stopped for the animal, the passive rotation was noted, and the animal was returned to its home cage. The rod and floor were wiped with alcohol between each test. On test-day, 2–3 trials and three actual tests were conducted for each mouse with a gap of 5 min between each test. The average time taken to fall from the rod on day (–1) is considered as 100% for each mouse. The percentage change duration to fall on the subsequent testing day is calculated and compared using the unpaired Student's *t*-test using Graphpad prism version 8.

### 2.6.6. ZIKV-NS1 antigen level as a measure of viral load

ZIKV-NS1 antigen levels in the serum were estimated using ZIKV-NS1 sandwich ELISA kit (BioFront Technologies) as an indirect estimation of viral load. Briefly, 5  $\mu$ l of the serum was diluted in 1:300 or 1:1500 in dilution buffer, added to antibody-coated plates, washed and HRP-labelled antibody added. Absorbance was read at 450 nm after the addition of substrate tetramethylbenzidine and stop solution. NS1 was quantified using the standard curve and multiplying by the dilution factor. Statistical analysis was done by unpaired Student's *t*-test using Graphpad prism version 8.

### 2.6.7. Viral copy number in serum

Serum stored at  $-70^{\circ}\text{C}$  was thawed, and 80  $\mu$ l of the serum was used to isolate RNA using QIAamp viral RNA mini kit (52,904 Qiagen). Briefly, the isolated RNA was converted into cDNA using Superscript III First-Strand synthesis (18080051 Invitrogen) and quantitative real time PCR was performed using SYBR Green PCR master mix (4,344,463 Invitrogen) and ZIKV specific primers (Supplementary Table 1, ZIKV-NS1-F & ZIKV-NS1-R). For the standard curve, the ZIKV viral RNA was synthesized *in vitro* and used in real-time PCR. The cycle threshold (Ct) values of the test samples were converted into viral copy numbers using the standard curve. Statistical analysis was done by unpaired Student's *t*-test using Graphpad prism version 8.

### 2.6.8. Ethics statement

The *in vivo* efficacy study in *Ifnar1*<sup>-/-</sup> mice was approved by the Institutional Animal Care and Use Committee of Florida State University and was in accordance with Public Health Service Policy and the Guide for the Care and Use of Laboratory Animals (8th edition).

## 3. Results

### 3.1. Purification of CST

The CST was purified from seeds of *C. australe* with an overall yield of 0.5%. As per the LCMS analysis, the purity was >98% and the NMR spectrum is shown in Supplementary Fig 1.

### 3.2. Viral load reduction and survivability in mice

In the initial study (mouse-study-I) in *ifnar1*<sup>-/-</sup> mice there was 46% ( $p = 0.003$ ) ZIKV-NS1 antigen level in serum and 68% ( $p = 0.011$ ) reduction of ZIKV-NS1 gene in liver tissue on day 3 dpi at CST 100 mg/kg dose given IP once daily (Fig. 1 D and Supplementary Fig 2A). We followed up this with a survivability study where mice were challenged with a ZIKV load of  $10^4$  ffu/mouse given IP at CST doses of 100 and 200 mg/kg once daily for a total of 7 doses (mouse-study-II). Consistent with the previous study, there was a significant decrease in the ZIKV-NS1 antigen level with CST 100 mg/kg ( $p = 0.018$ ) and 200 mg/kg ( $p = 0.038$ ) on day 3 dpi. (Supplementary Fig 3A). Additionally, there was a marginal increase in survivability ( $p = 0.044$ ) in the CST 200 mg/kg group, whereas in the lower dose of 100 mg/kg the difference in the survivability was not statistically significant (Supplementary Fig 3B). As the *ifnar1*<sup>-/-</sup> mouse is immunocompromised, a higher dose of the virus

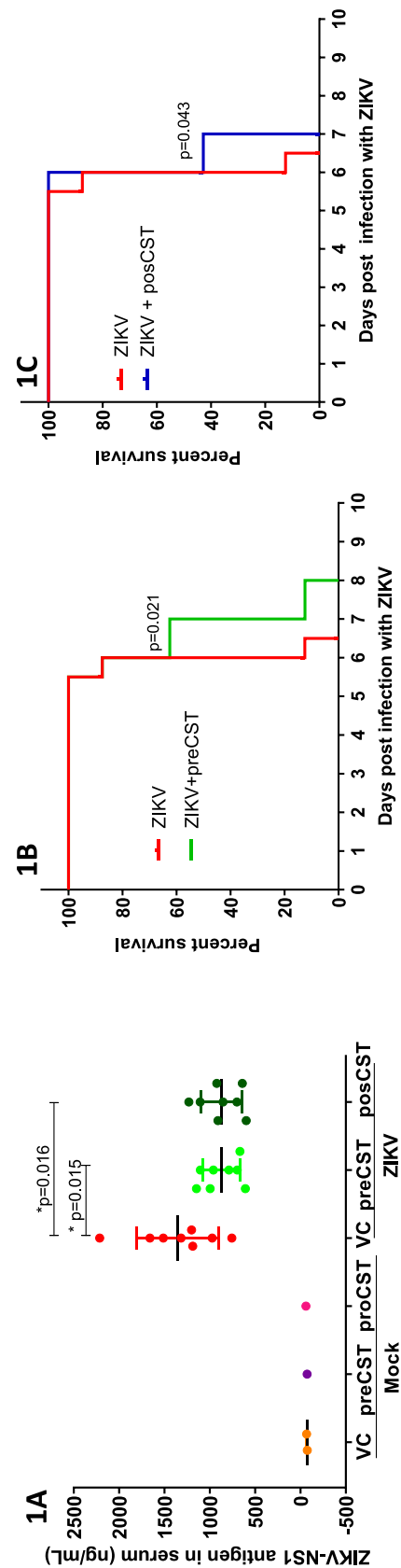


**Fig. 1.** CST improves survivability of ZIKV infected mouse marginally. The infection with ZIKV and treatment was done twice daily as explained in mouse –study-III. CST was given 100 mg/kg bw twice daily up to day 6 dpi. A survival blood sampling from tail was done on day 3 dpi. 1A: Viral load in serum was estimated by ELISA using ZIKV-NS1 kit. Statistical analysis was done by unpaired Student's *t*-test.  $p < 0.05$  is considered as significant. 1B and 1C: Survival curves of pretreatment (1 B) and post treatment (1 C) were plotted, Statistical analysis was done with the Kaplan Meier equation and comparison of survival curves was done using Log rank (Matmel-Cox) test using Graphpad prism version 8. dpi-days post infection.

may mask the efficacy of the test compounds, and hence ZIKV at a reduced dose ( $10^3$  ffu/mouse) was given IP in mouse-study-III. Also, to optimize the dose regime, instead of a single dose of 200 mg/kg, CST was given in split doses of 100 mg/kg/dose twice daily. We also wanted to determine the efficacy of CST when given post-infection. Hence, separate treatment groups were made wherein CST treatment started at 24 h before or 24 h after infection in mouse-study-III. Along with the 36% reduction in systemic viral load in serum taken from pre ( $p = 0.015$ ) and post ( $p = 0.016$ ) treatment groups on day 3 dpi (Fig. 1A), there was a marginal improvement in survival in both 24 h pre ( $p = 0.021$ ) and 24 h post ( $p = 0.043$ ) infection treatments (Fig. 1B and C). Pre-treatment of CST did not have any significant additional effect as compared to post-infection treatment. In mouse-study-IV, the ZIKV-NS1 antigen in the serum was estimated from day 2 to day 4 dpi, and the CST could inhibit the serum NS1 antigen levels from day 2 dpi (Fig. 2A). There was also a reduction of ZIKV-RNA copy number in the serum on day 4 dpi in both pre and post-infection treatments (Fig. 2B). Additionally, CST inhibited ZIKV-NS1 gene levels in tissues such as liver, spleen, and brain (Fig. 2C, D, 3C), indicating a decrease in the viral load.

### 3.3. Effect of CST on seizure, brain inflammation and motor co-ordination in ZIKV infected mice

When we analyzed the endpoints of survival studies, in mouse-study-II, four out of eight mice (50%) had hind limb paralysis, and 3 out of 8 (37%) had seizure. However, neither paralysis nor seizure was observed in CST 100 mg/kg, or 200 mg/kg treated infected mice (Table 3). Similarly, in mouse-study-III, the seizure and hind limb paralysis were observed in 40% and 50% of the ZIKV infected-untreated mice, respectively, as compared to none in CST treated-infected mice (Table 3). To reconfirm the above observations, a separate detailed

study (mouse-study-V) was conducted to see the effect of CST on neuronal abnormalities such as seizure and paralysis.

In mouse-study-V, mice were watched for unprovoked seizure from day 1–10 dpi by random observation and 1 h video recording on day 6 occurred when there was the first appearance of seizure while handling the mice. There was no unprovoked seizure observed in any of the mice. On day 6, some of the mice exhibited a seizure while opening the cage lid in ZIKV-infected untreated mice. To have a uniform provocation of seizure, a method was developed as described under “materials and methods” based on the previous observation. There was seizure in 50% of the untreated-infected mice ( $n = 8$ ) on day 6 dpi, whereas there was no seizure observed in CST treated mice on day 6 dpi (Fig. 3A). However, initial stages of neuronal abnormalities such as toe walking, and hunched positions were seen in a few of the mice (Table 4) CST treated mice. On day 7 dpi, out of the total infected mice, only 4 mice were surviving in CST treated groups. As the body weight decreased to 80% of starting weight, we euthanized these four mice as per the protocol. The uninfected mice were healthy and euthanized on day 10 dpi.

Further, to test the effect of ZIKV infection on motor neurons, the mice were subjected to the rotarod test. There was significant improvement in motor coordination in treated mice on day 3 ( $p = 0.036$ ,  $p = 0.006$  pre- and post-infection treatment, respectively), day 5 ( $p = 0.047$ ,  $p = 0.0005$  pre- and post-infection treatment) and on day 6 ( $p = 0.041$ ,  $p = 0.012$  pre- and post-infection treatment) dpi as measured by the rotarod test (Fig. 3B). In order to compare the muscle strength, we conducted an inverted grid suspension test. We did not see any difference in the time of fall between infected and untreated mice up to 120 s (Data not shown). There was no hind limb paralysis in any of the mice in mouse-study-V, and hence we could not analyze the effect of CST on paralysis in this study. However, data from the previous studies (mouse-study-II and mouse-study-III) indicate that there was no paralysis with

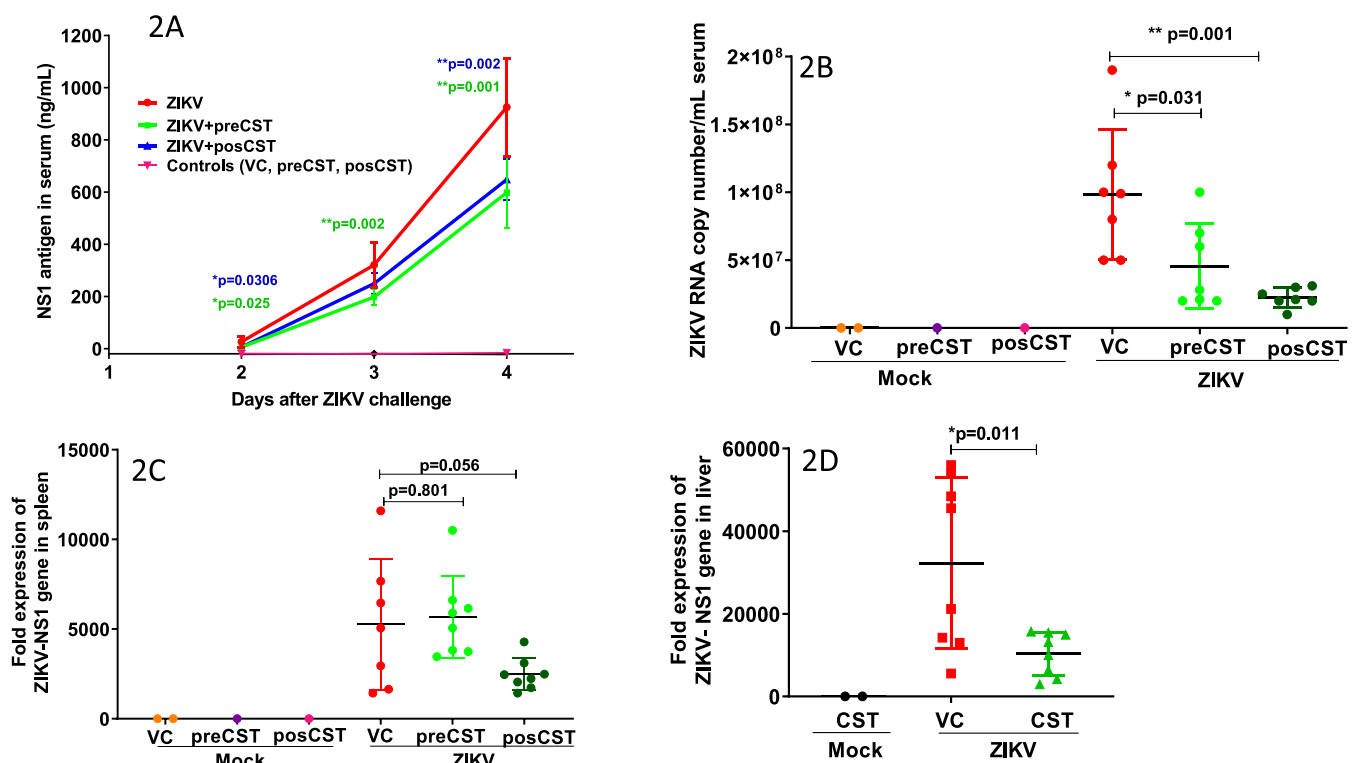


**Fig. 2.** CST inhibits systemic and tissue ZIKV load *in vivo*: *Ifnar1*<sup>-/-</sup> mice were treated with CST as explained in mouse-study-IV. Treatment with CST (100 mg/kg twice daily) started either 24 h before infection or 24 h after infection with ZIKV. A survival blood sampling was done from tail on day 2, 3, and 4 dpi. Mice were euthanized on day 4 dpi. Blood and tissue samples were collected. **2A:** ZIKV-NS1 antigen levels in serum on day 2, day 3 and day 4 dpi. **2B:** ZIKV RNA copy number in serum on day 4 dpi. **2C:** Expression level of ZIKV NS1 gene in spleen on day 4 dpi. **2D:** Mice were treated with CST as explained in Mouse study I. Relative expression of ZIKV NS1 in liver on day 3 dpi. Statistical analysis is done by unpaired students *t*-test using Graphpad prism version 8.  $p < 0.05$  is considered as significant.

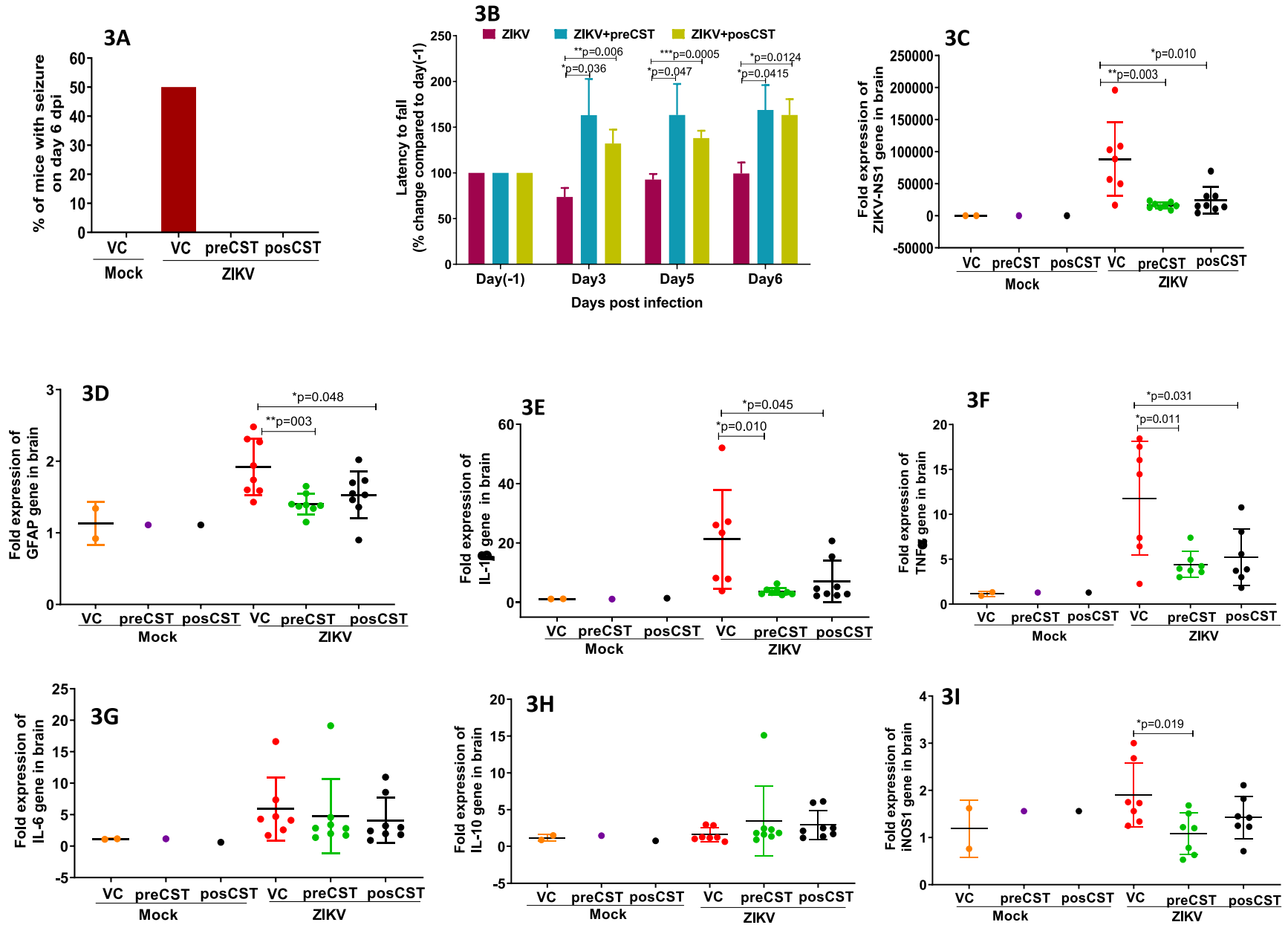


**Fig. 3.** Effect of CST on seizure and brain inflammation. *Ifnar1*<sup>-/-</sup> were treated with CST 100 mg/kg twice daily starting at 24 h before and 24 after the infection with ZIKV on day 0 as explained in mouse-study-V. Mice were observed for seizure or seizure related activities. **3A**: Mice with seizure **3B**: Motor coordination is assessed by rotarod test. The time taken to fall from the rod on day (-1) is taken as 100% for each mouse. Percentage change in the time is calculated for subsequent testing day. **3C–3I**: To check the effect of CST on inflammation of brain, the *ifnar1*<sup>-/-</sup> mice were treated and infected as explained in mouse-study-IV. RNA was extracted from the brain tissue, converted to cDNA, the relative expression levels of ZIKV-NS1 gene (**3C**), Astrocyte marker GFAP (**3D**), inflammation associated cytokines IL-1 $\beta$  (**3E**), TNF $\alpha$  (**3F**), IL-6 (**3G**), IL-10 (**3H**), inducible nitric oxide synthase iNOS1 (**3I**). Statistical analysis is done by unpaired Student's *t*-test.  $p < 0.05$  is considered as significant.

**Table 3**

Number of mice with seizures and paralysis. During survivability study, the reason for euthanizing the mice was noted. Hind limb paralysis and tremor were also the factors which determine end points. Seizures during opening of the cage in the morning were also noted. \*mice with at least one of the Racine stages of seizure and no video recording were done. \*\* Paralysis of at least one limb.

Mouse Study	Neuronal Disorder	Treatment groups		
		Saline + ZIKV	ZIKV+C100 mg/kg	ZIKV+C200 mg/kg
Mouse Study II	Seizure*	4/8 (50%)	0/8 (0%)	0/8 (0%)
	Hind limb paralysis**	3/8 (37%)	0/8 (0%)	0/8 (0%)
Mouse Study III	Seizure*	3/8 (40%)	–	0/8 (0%)
	Hind limb paralysis**	4/8 (50%)	–	0/8 (0%)

**Table 4**

Castanospermine abolishes or delays ZIKV induced seizure or related activities. In mouse study V, mice were observed before and after opening the cage lid for behaviour, body position, activities and scored accordingly. Mice were lifted by its tail and dropped to cage bed from a height of 30 cm three times. Seizure related activities were noted.

Seizure stages	Number of mice showing seizure related activities			
	Mock infection (n = 4)	ZIKV (n = 8)	ZIKV +posCas (n = 8)	ZIKV+preCas (n = 7)
Toe walking	0	7	0	1
Hunched dorsal	0	3	1	0
Erratic running	0	1	0	0
Jumping upon touching	0	2	0	0
Mouth and facial movement (RS-1)	0	4	0	0
Head nodding (RS-2)	0	3	0	0
Fore limb clonus (RS-3)	0	3	0	0
Rearing with forelimb clonus (RS-4)	0	1	0	0
Rearing and falling with forelimb clonus (RS-5)	0	1	0	0

RS- Racine scale.

#### CST treatment (Table 3).

Brain inflammation is one of the known causes of meningitis. We examined the expression levels of inflammation markers in the brain tissues collected on day 4 dpi of mouse-study-IV. Treatment with CST reduced ZIKV-NS1 gene levels in brain tissue (Fig. 3C). With ZIKV infection, there was also an increase in the mRNA of GFAP, an astrocyte marker (Fig. 3D), and inflammatory cytokines IL-1B, and TNF $\alpha$  and CST reduced the gene expression levels of these inflammatory markers (Fig. 3E and G). There was a small increase of IL-6 with ZIKV infection, but CST did not affect IL-6 mRNA levels (Fig. 3G). No change was seen in anti-inflammatory cytokine IL-10 with ZIKV infection or CST treatment (Fig. 3H). There was a slight increase in inducible nitric oxide synthase (iNOS1) gene in a few of the mice, and treatment with CST was able to inhibit iNOS1 in pre-treatment groups.

#### 3.4. In vitro toxicity and efficacy studies

First, we checked the cytotoxicity of CST to SNB19 cells. CST is well tolerated by SNB19 cells up to 3 mM and was toxic to SNB19 cells only at high concentration (CC<sub>50</sub> 153 mM) as measured by ATP content (Fig. 4A). Then we checked the anti-viral efficacy of CST in SNB19 cells against three different strains of ZIKV by focus forming assay. CST could

inhibit all three strains of ZIKV. CST had an IC<sub>50</sub> of 117.2  $\pm$  49  $\mu$ M in FSS13025, 98.02  $\pm$  43.81  $\mu$ M in MR766 and 78.49  $\pm$  28.19  $\mu$ M in, PRVABC59 strains (Fig. 4B–D). With CST, there was a dose-dependent decrease in the NS1 antigen levels as confirmed by Western blot (Fig. 4E).

#### 4. Discussion

Zika viral disease has become a concern because of its effect on neuronal tissues both in new-born children and adults. Attempts have been made to repurpose or develop anti-virals that can reduce the viral load. ZIKV infection is associated with neuronal abnormalities such as microcephaly, GBS, and seizures in clinical as well as experimental animal models. Encephalitis (inflammation of the brain), meningitis (Inflammation of membrane covering the brain), and myelitis (inflammation of spinal cord) are known to cause seizures. ZIKV infection causes encephalitis (Hayashida et al., 2019). We thought that CST, with its anti-viral and anti-inflammatory activity, can be useful in reducing the seizure-related neuronal disorders apart from viral load reduction and, thus, the severity of the infection. Dosing (IP) of rats with CST was able to decrease the  $\alpha$ -glucosidase activity in the brain (Saul et al., 1985), indicating that the CST is permeable to the brain-blood barrier.

$\alpha$ -Glucosidase is a host enzyme that removes glucose units from N-linked glycans and thereby participates in the maturation and folding of flaviviral glycoproteins (Courageot et al., 2000). CST, an  $\alpha$ -glucosidase inhibitor, is known for its anti-viral activity (Sayce et al., 2016; Taylor et al., 1994; Warfield et al., 2017; Whitby et al., 2004). The CST pro-drug celgosivir has better pharmacokinetics compared to CST, and clinical trials indicate that the CST-prodrug celgosivir is not having any known adverse effects (Sung et al., 2016). We explored the anti-viral and anti-inflammatory properties of CST to combat ZIKV infection *in vivo* in Ifnar1<sup>-/-</sup> mouse model and *in vitro* in SNB19 cells.

Ifnar1<sup>-/-</sup> mouse model does not have active IFN  $\alpha/\beta$  signalling, which is one of the major anti-viral pathways. Due to this reason, the Ifnar1<sup>-/-</sup> is highly susceptible to ZIKV and even adult mice when infected IP can give consistent mortality rates (Marzi et al., 2018). We have used Asian lineage of ZIKV (FSS13025), which is the lineage that has spread to the Americas and has raised serious concerns about human ZIKV-induced brain dysfunctions (Pol et al., 2017).

##### 4.1. Reduction of viral load and improvement in survivability

We have estimated ZIKV-NS1 antigen levels in the blood as an indirect measure of viral load due to the limited availability of blood samples in a survival blood sampling from the tail vein. NS1 antigen level correlated significantly with viremia in dengue patients (Duong et al., 2011). In another study where Ifnar1<sup>-/-</sup> mice were injected with ZIKV intraperitoneally, the viremia peaks were on 2–4 days post-infection (Aliota et al., 2016) which is in correlation with our results on ZIKV-NS1 antigenemia (Fig. 2A) and in our previously published data (Yang et al., 2018). In mouse-study-IV there was significant positive correlation (Pearson  $r = 0.66$ ,  $p = 0.0004$ ) between ZIKV-NS1 antigen levels and ZIKV-RNA copy number in blood (Supplementary Fig 4A).

In our initial studies, the treatment with CST was started the same time as that of ZIKV challenge, and there was a reduction in viral load both at the systemic level and tissue level as measured by secreted ZIKV-NS1 antigen and ZIKV-NS1 gene expression respectively. The reduction of viral load was observed even after CST treatment started 24 h post-infection. Pre-treatment of CST did not have a significant additional advantage over the post-treatment. This may be because the CST acts predominantly post-translationally affecting the proper glycosylation as compared to the entry-level of the virus. However, glycosylated moieties are important for host viral interaction too. Host cell surface glycans correlated strongly with the glycomic features of ZIKV E protein indicating ZIKV uses glycosylation of its E protein to interact with host cell receptors to facilitate entry (Routhu et al., 2019). High-throughput

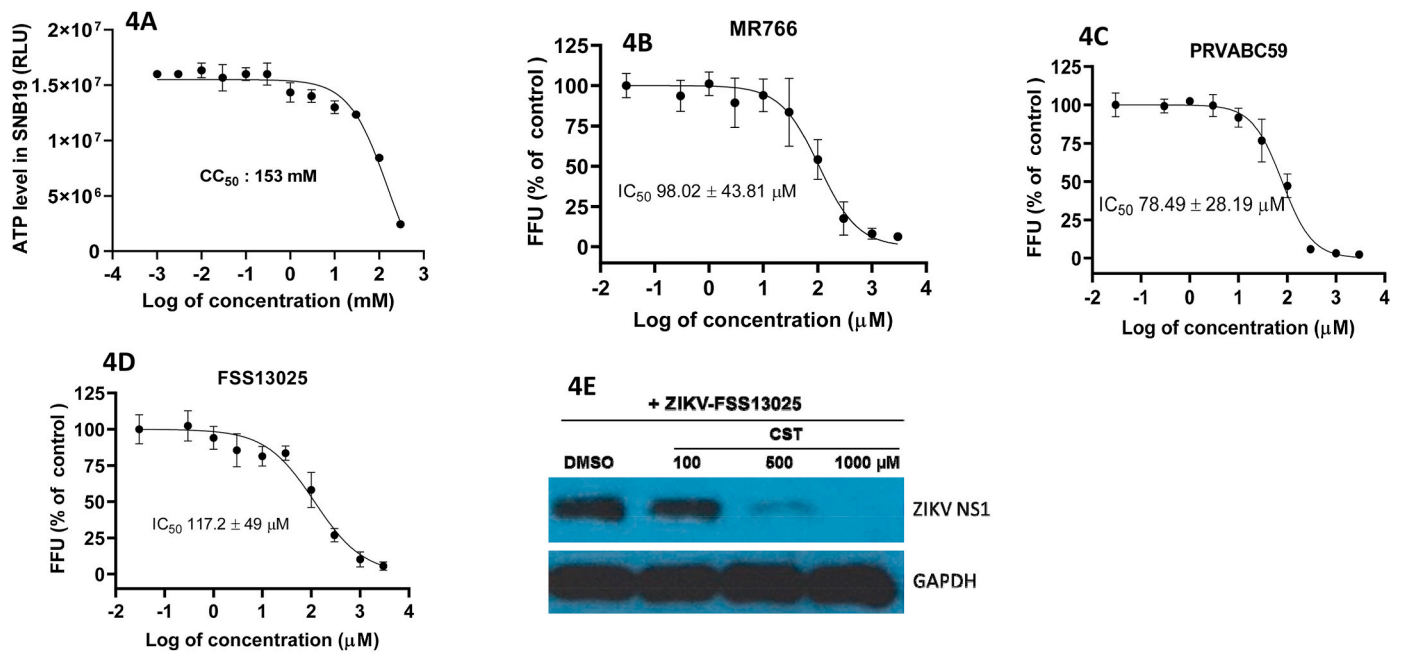


**Fig. 4.** CST inhibits Zika virus *in vitro* in glial cells. **4A.** Cytotoxicity of CST. SNB19 cells were treated with CST (0.0003–300 mM) for 24 h and ATP levels were estimated as relative luminescence units (RLU) using CellTiter Glo kit from Promega. **4B–4D:** Efficacy of CST in inhibiting various strains of ZIKV. SNB19 cells were seeded in 96 well plates and infected with ZIKV strains (MOI = 1) for 24 h. ZIKV load in culture supernatants were titered on Vero E6 cells by focus forming assay. Percentage of focus forming units (ffu) compared to DMSO control is calculated. CC50 and IC50 were calculated using Graphpad prism version 8. IC50 values are average of two repeats  $\pm$  standard deviation. **4E:** ZIKV-NS1 protein levels in SNB19 cells as tested by Western blot with glyceraldehyde 3-phosphate dehydrogenase (GAPDH) as loading control.

fitness profiling of ZIKV E protein reveals different roles for glycosylation during infection of mammalian and mosquito cells (Gong et al., 2018). Interference in the processes of glycosylation can generate non-infectious viral particles without decreasing the viral RNA. We have shown that treatment with CST has systemic viral RNA levels *in vivo*. When CST was given a single dose per day, at 200 mg/kg, there was an only marginal improvement in survivability. A split dose of CST (Watanabe et al., 2012) and an optimized dose regime can improve CST efficacy (Sung et al., 2016). Next, we tried to optimize the dose regime by dosing the mice 100 mg/kg twice daily instead of a single dose of 200 mg/kg per day. From two different studies, it indicates that split-dose did not have significant improvement in survivability as compared to a single dose. The level of survivability may also depend on the mouse model used in the study. In immunocompetent A/J mice infected with another member of flavivirus, dengue virus (DEN-2) injected intracranially; there was 90% survivability with 50 mg/kg CST (Whitby et al., 2005).

We also demonstrated the anti-ZIKV activity of CST *in vitro* in SNB19 cells using Western blot and focus forming assay. The CST could inhibit all the three strains of ZIKV in focus forming assay, although the potency is less *in vitro*. CST was tolerable to SNB19 and was toxic to cells only at high concentrations. The CC<sub>50</sub> of castanospermine and celgosivir in MDBK cells was >1000  $\mu$ M (Whitby et al., 2004).

#### 4.2. Reduction in brain inflammation and related neurological abnormalities

Following ZIKV infection, neurological abnormalities were reported in mouse models (Figueiredo et al., 2019) as well as in clinical conditions (Capasso et al., 2019; Moura da Silva et al., 2016). In our initial studies, we observed seizure in ZIKV infected mice while handling it, but not in CST treated ones. Moreover, none of the CST treated mice had hind limb paralysis giving us an indication that the CST may play a role in the reduction of neuronal abnormalities. As inflammation of the brain known to cause seizures, we studied, ZIKV induced inflammation of the

brain and effect of CST on seizure-related activity and other neurological disorders such as paralysis and motor co-ordination.

Apart from systemic inflammation, ZIKV cause inflammation of brain (Vieira et al., 2018) human retinal pigment epithelium (Simonin et al., 2019), ovary (Caine et al., 2019). Inflammation and seizure-like activities may not be specific to ZIKV, as it is also reported in immunocompromised mice infected with DENV too (Getts et al., 2007; Tsai et al., 2016). The inflammation might be a common factor that cause seizures. Apart from immunocompetent neonatal mice, ZIKV induced seizures were also reported in immunocompromised adult mice (Zukor et al., 2018). In our study, the immunocompromised adult mice (6–7 wk old) show seizure in 40–50% of infected untreated mice while handling them, and hence we considered it as provoked seizures. Spontaneous seizures were reported when 3-day old Swiss mice were infected with ZIKV 10<sup>6</sup> ffu/mouse (Souza et al., 2018). They also observed increased susceptibility to chemically induced seizures in adult mice. However, in our studies with adult mice, we did not observe the spontaneous seizures during random observation and during 1 h video recording on day 6 dpi.

CST is also known for its immunosuppressive properties (Bartlett et al., 1994; den Dulk et al., 2004). CST inhibited passively induced allergic encephalomyelitis in a dose-dependent manner when administered continuously for 7 days, beginning at the time of lymphocyte transfer (Willenborg et al., 1989). In our study, ZIKV infected mice have shown an increase in inflammatory marker genes, mainly IL-1 $\beta$  and TNF $\alpha$  on day 4 dpi. Treating with CST has reduced the level of these cytokine genes in the brain. In dengue patients, the TNF $\alpha$  was reduced following treatment with celgosivir (Sung et al., 2016). There was an increase in expression GFAP gene, an astrocyte marker indicating infiltration of astrocytes or changes in expression pattern. Astrocytes induce neuroinflammation through pro-inflammatory cytokines mediating synaptic and cognitive changes (Stefanik et al., 2018). Although there is an increase in gene expression of IL-6 with ZIKV infection, no reduction was observed with CST treatment. No changes were observed in the gene expression of anti-inflammatory cytokine IL-10 with ZIKV infection. Carbohydrate moieties play an important role in some critical steps of

the neuro-immunologic inflammatory process of allergic encephalomyelitis, and CST inhibited passively induced allergic encephalomyelitis in a dose-dependent manner (Willenborg et al., 1989). Blocking of TNF $\alpha$  using neutralizing monoclonal antibodies prevented seizures in young Swiss mice and normalizes susceptibility to chemically induced seizures in adult mice submitted to neonatal ZIKV infection (Souza et al., 2018). Acute myelitis due to ZIKV infection was reported in a 15-year old girl, and treatment with immunosuppressant drug methylprednisolone for 7 days improved her neurological condition (M  charles et al., 2016).

Along with inflammatory markers, there was an increase in iNOS1 mRNA expression in ZIKV infected mice, and CST was able restore the normal level in pre-infection treatment mice, although it was not statistically significant in post-infection treatment of mice. Early in the course of systemic inflammation, there is a profound induction of iNOS mRNA in vascular, glial and neuronal structures of the rat brain, accompanied by the production of nitric oxide metabolites in the brain parenchyma and cerebrospinal fluid (Wong et al., 1996).

The reduction in brain inflammation can be either due to an overall reduction in viral load or a combined effect of anti-viral and immunosuppressive activity of CST. Although the group size is small ( $n = 2$ ), CST did not suppress the basal level of inflammation in control mice, which were not infected. Iminosugar N-butyl-1-deoxynojirimycin and N-(9-methoxynonyl-1-DNJ) counteracted IFN $\gamma$ /R, which is down-regulated by DENV infection in human monocyte-derived macrophages (Miller et al., 2019). Hence, CST might play anti-viral activity at various stages of ZIKV infection.

Inhibition of glucose trimming with CST promoted degradation of the alpha subunit of the nicotinic acetylcholine receptor (nAChR) (Keller et al., 1998). Although not tested, another possible mechanism by which the CST reduces seizure may be by inhibiting the nAChR, which is an excitatory ligand-gated channel.

From mouse-study-II and mouse-study-III, it is clear that the CST treatment could delay hind limb paralysis. The hind limb paralysis observed in ZIKV infection of ifnar1<sup>-/-</sup> mice may be the result of infection and inflammation in motor neurons. In our study, we found the motor dysfunction in ZIKV infected mice, as demonstrated by the rotarod test. The CST treated mice could remain on the rod for a more extended period as compared to untreated ones. The grip strength test is a widely used non-invasive method designed to evaluate mouse limb strength that has been used to investigate the effects of neuromuscular disorders and the effect of drugs. Inverted grid suspension test measures the ability of the mouse to hang on a mesh with its forepaws for a pre-set length of time or until grip fails. We assessed grip strength for 2 min, and all the mice could complete 2 min irrespective of ZIKV infection or CST treatment.

In conclusion, we have reported anti-ZIKV activity of CST *in vivo*. Moreover, CST abolished inflammation-mediated neuronal abnormalities such as seizure and paralysis till day 7 dpi. Since, we must euthanize the mice on day 7 dpi because of the bodyweight loss; we do not have data for subsequent days and hence further studies may require to understand whether CST can abolish or delay the seizure. Although there are reports of a few clinical trials about the anti-viral efficacy of CST-prodrug celgosivir, no report of clinical trials on effectiveness of CST or celgosivir on neuronal abnormalities such as seizure and paralysis. The combined anti-viral and anti-inflammatory properties of castanospermine are possibly effective in treating neuronal disorders in ZIKV infection. Hence, it will be worth testing the pro-drug celgosivir for control of seizure-related issues in ZIKV infection, either alone or in combination with other potent anti-virals. The combinational therapy of anti-viral and anti-inflammatory drugs is gaining importance as a new strategy in the treatment of many viral diseases, including COVID-19.

#### Authors' contributions

A.M.T., H.T., E.H.H., G.K.O Design the study and wrote the manuscript, A.M.T. and Y.C. conducted the study, E.H.H. extraction and

purification of castanospermine.

#### Declaration of competing interest

The authors declare that they have no conflict of interest.

#### Acknowledgements

The authors thank Dr. Kathleen Harper for her guidance in in-vivo studies. Suggestions from Dr. Sanjay Kumar for seizure studies are greatly appreciated. Help from Jason Nipper in the animal room maintenance is gratefully acknowledged. Support from Dr. Brian K. Washburn and Kristina Poduch in performing PCR of samples is appreciated. The study is supported by Zika seed funding to H.T. from Florida State University Office of Research.

#### Appendix A. Supplementary data

Supplementary data to this article can be found online at <https://doi.org/10.1016/j.antiviral.2020.104935>.

#### References

- Aliota, M.T., Caine, E.A., Walker, E.C., Larkin, K.E., Camacho, E., Osorio, J.E., 2016. Characterization of lethal zika virus infection in AG129 mice. *PLoS Neglected Trop. Dis.* 10, e0004682 <https://doi.org/10.1371/journal.pntd.0004682>.
- Allison, S.L., Stadler, K., Mandl, C.W., Kunz, C., Heinz, F.X., 1995. Synthesis and secretion of recombinant tick-borne encephalitis virus protein E in soluble and particulate form. *J. Virol.* 69, 5816–5820.
- Annamalai, A.S., Pattanaik, A., Sahoo, B.R., Guinn, Z.P., Bullard, B.L., Weaver, E.A., Steffen, D., Natarajan, S.K., Petro, T.M., Pattanaik, A.K., 2019. An attenuated zika virus encoding non-glycosylated envelope (E) and non-structural protein 1 (NS1) confers complete protection against lethal challenge in a mouse model. *Vaccines* 7, 112. <https://doi.org/10.3390/vaccines7030112>.
- Asadi-Pooya, A.A., 2016. Zika virus-associated seizures. *Seizure - Eur. J. Epilepsy* 43, 13. <https://doi.org/10.1016/j.seizure.2016.10.011>.
- Barker-Haliski, M.L., Heck, T.D., Dahle, E.J., Vanegas, F., Pruess, T.H., Wilcox, K.S., White, H.S., 2016. Acute treatment with minocycline, but not valproic acid, improves long-term behavioral outcomes in the Theiler's virus model of temporal lobe epilepsy. *Epilepsia* 57. <https://doi.org/10.1111/epi.13577>, 1958–1967.
- Bartlett, M.R., Warren, H.S., Cowden, W.B., Parish, C.R., 1994. Effects of the anti-inflammatory compounds castanospermine, mannose-6-phosphate and fucoidan on allograft rejection and elicited peritoneal exudates. *Immunol. Cell Biol.* 72, 367–374. <https://doi.org/10.1038/icb.1994.55>.
- Brasil, P., Sequeira, P.C., Freitas, A.D., Zogbi, H.E., Calvet, G.A., Souza, R.V., de Siqueira, A.M., Mendonca, M.C.L. de, Nogueira, R.M.R., Filippis, A.M.B. de, Solomon, T., 2016. Guillain-Barr   syndrome associated with Zika virus infection. *Lancet* 387, 1482. [https://doi.org/10.1016/S0140-6736\(16\)30058-7](https://doi.org/10.1016/S0140-6736(16)30058-7).
- Caine, E.A., Scheaffer, S.M., Broughton, D.E., Salazar, V., Govero, J., Poddar, S., Osula, A., Halabi, J., Skaznik-Wikiel, M.E., Diamond, M.S., Moley, K.H., 2019. Zika virus causes acute infection and inflammation in the ovary of mice without apparent defects in fertility. *J. Infect. Dis.* 220, 1904–1914. <https://doi.org/10.1093/infdis/jiz239>.
- Cao-Lormeau, V.-M., Blake, A., Mons, S., Last  re, S., Roche, C., Vanhomwegen, J., Dub, T., Baudouin, L., Teissier, A., Larre, P., Vial, A.-L., Decam, C., Choumet, V., Halstead, S.K., Willison, H.J., Musset, L., Manuguerra, J.-C., Despres, P., Fournier, E., Mallet, H.-P., Musso, D., Fontanet, A., Neil, J., Ghawch  re, F., 2016. Guillain-Barr   Syndrome outbreak associated with Zika virus infection in French Polynesia: a case-control study. *Lancet* 387, 1531–1539. [https://doi.org/10.1016/S0140-6736\(16\)00562-6](https://doi.org/10.1016/S0140-6736(16)00562-6).
- Capasso, A., Ompad, D.C., Vieira, D.L., Wilder-Smith, A., Tozan, Y., 2019. Incidence of Guillain-Barr   Syndrome (GBS) in Latin America and the Caribbean before and during the 2015–2016 Zika virus epidemic: a systematic review and meta-analysis. *PLoS Neglected Trop. Dis.* 13, e0007622 <https://doi.org/10.1371/journal.pntd.0007622>.
- Caputo, A.T., Alonzi, D.S., Marti, L., Reca, I.-B., Kiappes, J.L., Struwe, W.B., Cross, A., Basu, S., Lowe, E.D., Darlot, B., Santino, A., Roversi, P., Zitzmann, N., 2016. Structures of mammalian ER  $\alpha$ -glucosidase II capture the binding modes of broad-spectrum iminosugar antivirals. *Proc. Natl. Acad. Sci. Unit. States Am.* 113, E4630–E4638. <https://doi.org/10.1073/pnas.1604463113>.
- Chang, J., Block, T.M., Guo, J.-T., 2013a. Antiviral therapies targeting host ER alpha-glucosidases: current status and future directions. *Antivir. Res.* 99, 251–260. <https://doi.org/10.1016/j.antiviral.2013.06.011>.
- Chang, J., Guo, J.-T., Du, Y., Block, T., 2013b. Imino sugar glucosidase inhibitors as broadly active anti-filovirus agents. *Emerg. Microb. Infect.* 2, 1–7. <https://doi.org/10.1038/emi.2013.77>.
- Courageot, M.-P., Frenkiel, M.-P., Duarte Dos Santos, C., Deubel, V., Despr  s, P., 2000.  $\alpha$ -Glucosidase inhibitors reduce dengue virus production by affecting the initial steps of virion morphogenesis in the endoplasmic reticulum. *J. Virol.* 74, 564–572.

- Crabtree, M.B., Kinney, R.M., Miller, B.R., 2005. Deglycosylation of the NS1 protein of dengue 2 virus, strain 16681: construction and characterization of mutant viruses. *Arch. Virol.* 150, 771–786. <https://doi.org/10.1007/s00705-004-0430-8>.
- Darbellay, J., Cox, B., Lai, K., Delgado-Ortega, M., Wheler, C., Wilson, D., Walker, S., Starrak, G., Hockley, D., Huang, Y., Mutwiri, G., Potter, A., Gilmour, M., Safronetz, D., Gerds, V., Karniychuk, U., 2017. Zika virus causes persistent infection in porcine conceptuses and may impair health in offspring. *EBioMedicine* 25, 73–86. <https://doi.org/10.1016/j.ebiom.2017.09.021>.
- Deacon, R.M.J., 2013. Measuring motor coordination in mice. *JoVE J. Vis. Exp.* <https://doi.org/10.3791/2609>.
- Dejnirattisai, W., Supasa, P., Wongwiwat, W., Rouvinski, A., Barba-Spaeth, G., Duangchinda, T., Sakuntabhai, A., Cao-Lormeau, V.-M., Malasit, P., Rey, F.A., Mongkolsapaya, J., Screaton, G.R., 2016. Dengue virus sero-cross-reactivity drives antibody-dependent enhancement of infection with zika virus. *Nat. Immunol.* 17, 1102–1108. <https://doi.org/10.1038/ni.3515>.
- den Dulk, M., Wang, C., Li, J., Clark, D.A., Hibberd, A.D., Terpstra, O.T., McCaughan, G. W., Bishop, G.A., 2004. Combined donor leucocyte administration and immunosuppressive drug treatment for survival of rat heart allografts. *Transpl. Immunol.* 13, 177–184. <https://doi.org/10.1016/j.trim.2004.05.003>.
- Dowall, S.D., Graham, V.A., Rayner, E., Atkinson, B., Hall, G., Watson, R.J., Bosworth, A., Bonney, L.C., Kitchen, S., Hewson, R., 2016. A susceptible mouse model for zika virus infection. *PLoS Neglected Trop. Dis.* 13.
- Duong, V., Ly, S., Lorn Try, P., Tuiskunen, A., Ong, S., Chroeing, N., Lundkvist, A., Leparcoffart, I., Deubel, V., Vong, S., Buchy, P., 2011. Clinical and virological factors influencing the performance of a NS1 antigen-capture assay and potential use as a marker of dengue disease severity. *PLoS Neglected Trop. Dis.* 5 <https://doi.org/10.1371/journal.pntd.0001244>.
- Dwek, R.A., Butters, T.D., Platt, F.M., Zitzmann, N., 2002. Targeting glycosylation as a therapeutic approach. *Nat. Rev. Drug Discov.* 1, 65–75. <https://doi.org/10.1038/nrd708>.
- Elbein, A.D., 1991. Glycosidase inhibitors: inhibitors of N-linked oligosaccharide processing. *Faseb. J.* 5, 3055–3063. <https://doi.org/10.1096/fasebj.5.15.1743438>.
- Elshuber, S., Allison, S.L., Heinz, F.X., Mandl, C.W., 2003. Cleavage of protein prM is necessary for infection of BHK-21 cells by tick-borne encephalitis virusFN1. *J. Gen. Virol.* 84, 183–191. <https://doi.org/10.1099/vir.0.18723-0>.
- Figueiredo, C.P., Barros-Aragão, F.G.Q., Neris, R.L.S., Frost, P.S., Soares, C., Souza, I.N. O., Zeidler, J.D., Zamberlan, D.C., de Sousa, V.L., Souza, A.S., Guimarães, A.L.A., Bellio, M., Marcondes de Souza, J., Alves-Leon, S.V., Neves, G.A., Paula-Neto, H.A., Castro, N.G., De Felice, F.G., Assunção-Miranda, I., Clarke, J.R., Da Poian, A.T., Ferreira, S.T., 2019. Zika virus replicates in adult human brain tissue and impairs synapses and memory in mice. *Nat. Commun.* 10, 3890. <https://doi.org/10.1038/s41467-019-11866-7>.
- Fontes-Garfias, C.R., Shan, C., Luo, H., Muruato, A.E., Medeiros, D.B.A., Mays, E., Xie, X., Zou, J., Roundy, C.M., Wakamiya, M., Rossi, S.L., Wang, T., Weaver, S.C., Shi, P.-Y., 2017. Functional analysis of glycosylation of zika virus envelope protein. *Cell Rep.* 21, 1180–1190. <https://doi.org/10.1016/j.celrep.2017.10.016>.
- Getts, D.R., Matsumoto, I., Müller, M., Getts, M.T., Radford, J., Shrestha, B., Campbell, I. L., King, N.J.C., 2007. Role of IFN- $\gamma$  in an experimental murine model of West Nile virus-induced seizures. *J. Neurochem.* 103, 1019–1030. <https://doi.org/10.1111/j.1471-4159.2007.04798.x>.
- Gong, D., Zhang, T.-H., Zhao, D., Du, Y., Chapa, T.J., Shi, Y., Wang, L., Contreras, D., Zeng, G., Shi, P.-Y., Wu, T.-T., Arumugaswami, V., Sun, R., 2018. High-throughput fitness profiling of zika virus E protein reveals different roles for glycosylation during infection of mammalian and mosquito cells. *iScience* 1, 97–111. <https://doi.org/10.1016/j.isci.2018.02.005>.
- Hayashida, E., Ling, Z.L., Ashhurst, T.M., Viengkhou, B., Jung, S.R., Songkhunawej, P., West, P.K., King, N.J.C., Hofer, M.J., 2019. Zika virus encephalitis in immunocompetent mice is dominated by innate immune cells and does not require T or B cells. *J. Neuroinflammation* 16, 177. <https://doi.org/10.1186/s12974-019-1566-5>.
- Heinz, F.X., Auer, G., Stiasny, K., Holzmann, H., Mandl, C., Guirakhoo, F., Kunz, C., 1994. The interactions of the flavivirus envelope proteins: implications for virus entry and release. In: Brinton, M.A., Calisher, C.H., Rueckert, R. (Eds.), *Positive-Strand RNA Viruses, Archives of Virology Supplementum*. Springer, Vienna, pp. 339–348. [https://doi.org/10.1007/978-3-7091-9326-6\\_34](https://doi.org/10.1007/978-3-7091-9326-6_34).
- Hohenschütz, L.D., Bell, E.A., Jewess, P.J., Leworthy, D.P., Pryce, R.J., Arnold, E., Clardy, J., 1981. Castanospermine, A 1,6,7,8-tetrahydroxyoctahydroindolizine alkaloid, from seeds of *Castanospermum australe*. *Phytochemistry* 20, 811–814. [https://doi.org/10.1016/0031-9422\(81\)85181-3](https://doi.org/10.1016/0031-9422(81)85181-3).
- Kassavetis, P., Joseph, J.-M.B., Francois, R., Perloff, M.D., Berkowitz, A.L., 2016. Zika virus-associated Guillain-Barré syndrome variant in Haiti. *Neurology* 87, 336–337. <https://doi.org/10.1212/WNL.0000000000002759>.
- Keller, S.H., Lindstrom, J., Taylor, P., 1998. Inhibition of glucose trimming with castanospermine reduces calnexin association and promotes proteasome degradation of the  $\alpha$ -subunit of the nicotinic acetylcholine receptor. *J. Biol. Chem.* 273, 17064–17072. <https://doi.org/10.1074/jbc.273.27.17064>.
- Lazear, H.M., Govero, J., Smith, A.M., Platt, D.J., Fernandez, E., Miner, J.J., Diamond, M. S., 2016. A mouse model of zika virus pathogenesis. *Cell Host Microbe* 19, 720–730. <https://doi.org/10.1016/j.chom.2016.03.010>.
- Li, P.-C., Jang, J., Hsia, C.-Y., Groomes, P.V., Lian, W., de Wispelaere, M., Pitts, J.D., Wang, J., Kwiatkowski, N., Gray, N.S., Yang, P.L., 2019. Small molecules targeting the flavivirus E protein with broad-spectrum activity and antiviral efficacy in vivo. *ACS Infect. Dis.* 5, 460–472. <https://doi.org/10.1021/acinfedcis.8b00322>.
- Lüttjohann, A., Fabene, P.F., van Luijtelaar, G., 2009. A revised Racine's scale for PTZ-induced seizures in rats. *Physiol. Behav.* 98, 579–586. <https://doi.org/10.1016/j.physbeh.2009.09.005>.
- Manangeeswaran, M., Ireland, D.D.C., Verthelyi, D., 2016. Zika (PRVABC59) infection is associated with T cell infiltration and neurodegeneration in CNS of immunocompetent neonatal C57BL/6 mice. *PLoS Pathog.* 12 <https://doi.org/10.1371/journal.ppat.1006004>.
- Marzi, A., Emanuel, J., Callison, J., McNally, K.L., Arndt, N., Chadinha, S., Martellaro, C., Rosenke, R., Scott, D.P., Safronetz, D., Whitehead, S.S., Best, S.M., Feldmann, H., 2018. Lethal Zika virus disease models in young and older interferon  $\alpha/\beta$  receptor knock out mice. *Front. Cell. Infect. Microbiol.* 8 <https://doi.org/10.3389/fcimb.2018.00117>.
- Mécharles, S., Herrmann, C., Poullain, P., Tran, T.-H., Deschamps, N., Mathon, G., Landais, A., Breurec, S., Lannuzel, A., 2016. Acute myelitis due to Zika virus infection. *Lancet* 387, 1481. [https://doi.org/10.1016/S0140-6736\(16\)00644-9](https://doi.org/10.1016/S0140-6736(16)00644-9).
- Miller, J.L., Hill, M.L., Brun, J., Pountain, A., Sayce, A.C., Zitzmann, N., 2019. Iminosugars counteract the downregulation of the interferon  $\gamma$  receptor by dengue virus. *Antivir. Res.* 170, 104551. <https://doi.org/10.1016/j.antiviral.2019.104551>.
- Mlakar, J., Korva, M., Tul, N., Popović, M., Poljšak-Prijatelj, M., Mraz, J., Kolenc, M., Resman Rus, K., Vesnaver Vipotnik, T., Fabjan Vodusek, V., Vizjak, A., Pizem, J., Petrovec, M., Avšič Županc, T., 2016. Zika virus associated with microcephaly. *N. Engl. J. Med.* 374, 951–958. <https://doi.org/10.1056/NEJMoa1600651>.
- Morrey, J.D., Oliveira, A.L.R., Wang, H., Zukor, K., de Castro, M.V., Siddharthan, V., 2019. Zika virus infection causes temporary paralysis in adult mice with motor neuron synaptic retraction and evidence for proximal peripheral neuropathy. *Sci. Rep.* 9, 19531. <https://doi.org/10.1038/s41598-019-55717-3>.
- Morton, D.B., 2000. A systematic approach for establishing humane endpoints. *ILAR J.* 41, 80–86. <https://doi.org/10.1093/ilar.41.2.80>.
- Moura da Silva, A.A., Ganz, J.S.S., Sousa, P. da S., Doriqui, M.J.R., Ribeiro, M.R.C., Branco, M. dos R.F.C., Queiroz, R.C. de S., Pacheco, M. de J.T., Vieira da Costa, F.R., Silva, F. de S., Simões, V.M.F., Pacheco, M.A.B., Lamy-Filho, F., Lamy, Z.C., Soares de Brito e Alves, M.T.S., 2016. Early growth and neurologic outcomes of infants with probable congenital zika virus syndrome. *Emerg. Infect. Dis.* 22, 1953–1956. <https://doi.org/10.3201/eid2211.160956>.
- Olfert, E.D., Godson, D.L., 2000. Humane endpoints for infectious disease animal models. *ILAR J.* 41, 99–104. <https://doi.org/10.1093/ilar.41.2.99>.
- Pastula, D.M., Smith, D.E., Beckham, J.D., Tyler, K.L., 2016. Four emerging arboviral diseases in North America: jamestown Canyon, Powassan, chikungunya, and Zika virus diseases. *J. Neurovirol.* 22, 257–260. <https://doi.org/10.1007/s13365-016-0428-5>.
- Perry, S.T., Buck, M.D., Plummer, E.M., Penmasta, R.A., Batra, H., Stavale, E.J., Warfield, K.L., Dwek, R.A., Butters, T.D., Alonzi, D.S., Lada, S.M., King, K., Klose, B., Ramstedt, U., Shrestha, S., 2013. An iminosugar with potent inhibition of dengue virus infection in vivo. *Antivir. Res.* 98, 35–43. <https://doi.org/10.1016/j.antiviral.2013.01.004>.
- Pessoa, A., Linden, V. van der, Yeargin-Allsopp, M., Carvalho, M.D.C.G., Ribeiro, E.M., Braun, K.V.N., Durkin, M.S., Pastula, D.M., Moore, J.T., Moore, C.A., 2018. Motor abnormalities and epilepsy in infants and children with evidence of congenital zika virus infection. *Pediatrics* 141, S167–S179. <https://doi.org/10.1542/peds.2017-2038F>.
- Petridou, C., Bonsall, D., Ahmed, A., Roberts, M., Bell, C., de Cesare, M., Bowden, R., Graham, V., Bailey, D., Simpson, A., Aarons, E., 2019. Prolonged zika virus RNA detection in semen of immunosuppressed patient. *Emerg. Infect. Dis.* 25, 1598–1600. <https://doi.org/10.3201/eid2508.181543>.
- Pol, A.N. van den, Mao, G., Yang, Y., Ornaghi, S., Davis, J.N., 2017. Zika virus targeting in the developing brain. *J. Neurosci.* 37, 2161–2175. <https://doi.org/10.1523/JNEUROSCI.3124-16.2017>.
- Pryor, M.J., Wright, P.J., 1994. Glycosylation mutants of dengue virus NS1 protein. *J. Gen. Virol.* 75, 1183–1187. <https://doi.org/10.1099/0022-1317-75-5-1183>.
- Rabl, R., Horvath, A., Breitschaedel, C., Flunkert, S., Roemer, H., Hutter-Paier, B., 2016. Quantitative evaluation of orofacial motor function in mice: the pasta gnawing test, a voluntary and stress-free behavior test. *J. Neurosci. Methods* 274, 125–130. <https://doi.org/10.1016/j.jneumeth.2016.10.006>.
- Racine, R.J., 1972. Modification of seizure activity by electrical stimulation: II. Motor seizure. *Electroencephalogr. Clin. Neurophysiol.* 32, 281–294. [https://doi.org/10.1016/0013-4694\(72\)90177-0](https://doi.org/10.1016/0013-4694(72)90177-0).
- Reyes, Y., Bowman, N.M., Becker-Dreps, S., Centeno, E., Collins, M.H., Liou, G.-J.A., Bucardo, F., 2019. Prolonged shedding of zika virus RNA in vaginal secretions, Nicaragua. *Emerg. Infect. Dis.* 25, 808–810. <https://doi.org/10.3201/eid2504.180977>.
- Rossi, S.L., Tesh, R.B., Azar, S.R., Muruato, A.E., Hanley, K.A., Auguste, A.J., Langsjoen, R.M., Paessler, S., Vasilakis, N., Weaver, S.C., 2016. Characterization of a novel murine model to study zika virus. *Am. J. Trop. Med. Hyg.* 94, 1362–1369. <https://doi.org/10.4269/ajtmh.16-0111>.
- Routhou, N.K., Lehoux, S.D., Rouse, E.A., Bidokhti, M.R.M., Giron, L.B., Anzurez, A., Reid, S.P., Abdel-Mohsen, M., Cummings, R.D., Byrreddy, S.N., 2019. Glycosylation of zika virus is important in host–virus interaction and pathogenic potential. *Int. J. Mol. Sci.* 20, 5206. <https://doi.org/10.3390/ijms20205206>.
- Rozé, B., Najjioullah, F., Fergé, J.-L., Dorléans, F., Apetse, K., Barnay, J.-L., Daudens-Vaysse, H., Brouste, Y., Césaire, R., Fagour, L., Valentino, R., Ledrans, M., Mehdaoui, H., Abel, S., Leparcoffart, I., Signate, A., Cabié, A., Abgrall, G.J., Aïm, V., Arrigo, A., Cabre, P., Chabartier, C., Colombani, S., Cuziat, J., Deligny, C., Desbois, N., Dessoy, A.-L., Dounoyer, G., Duvauferrier, R., Duc, N., Edimona, M., Garrigou, P., Gaucher, S., Gourgoudou, S., Guitteaud, K., Hochedez, P., Ivanès, G., Jacquens, Y., Julié, S., Jean-Etienne, A., Jeannin, S., Julien, J., Jérémie, P., Lamaignère, J.-L., Laudarin, I., Le Gall, M., Legris-Allussou, V., Mejdoubi, M., Michel, C., Michel, F., Miossec, C., Moinet, F., Minerva, C., Olive, C., Olive, P., Pailla, K., Paysant, C., Pierre-François, S., Pircher, M., Polomat, K., Putoat, A., René-Corail, P., Resiere, D., Richer, C., Risson, J.-R., Rome, K., Sabia, M., Schloesser, M.,

- Simonnet-Vigeral, P., Théodose, R., Vilain, R., 2017. Guillain-barré syndrome associated with zika virus infection in Martinique in 2016: a prospective study. *Clin. Infect. Dis.* 65, 1462–1468. <https://doi.org/10.1093/cid/cix588>.
- Rozé, B., Najjoulah, F., Signate, A., Apetse, K., Brouste, Y., Gourgoudou, S., Fagour, L., Abel, S., Hochedez, P., Cesaire, R., Cabié, A., Neuro-Zika Working Group of Martinique, 2016. Zika virus detection in cerebrospinal fluid from two patients with encephalopathy, Martinique. February 2016 Euro Surveill. *Bull. Eur. Sur Mal. Transm. Eur. Commun. Dis. Bull.* 21. <https://doi.org/10.2807/1560-7917.ES.2016.21.16.30205>.
- Saiz, J.-C., Oya, N.J. de, Blázquez, A.-B., Escibano-Romero, E., Martín-Acebes, M.A., 2018. Host-directed antivirals: a realistic alternative to fight zika virus. *Viruses* 10, 453. <https://doi.org/10.3390/v10090453>.
- Saul, R., Ghidoni, J.J., Molyneux, R.J., Elbein, A.D., 1985. Castanospermine inhibits alpha-glucosidase activities and alters glycogen distribution in animals. *Proc. Natl. Acad. Sci. Unit. States Am.* 82, 93–97. <https://doi.org/10.1073/pnas.82.1.93>.
- Sayce, A.C., Alonzi, D.S., Killingbeck, S.S., Tyrrell, B.E., Hill, M.L., Caputo, A.T., Iwaki, R., Kinami, K., Ide, D., Kiappes, J.L., Beatty, P.R., Kato, A., Harris, E., Dwek, R. A., Miller, J.L., Zitzmann, N., 2016. Iminosugars inhibit dengue virus production via inhibition of ER alpha-glucosidases—not glycolipid processing enzymes. *PLoS Neglected Trop. Dis.* 10 <https://doi.org/10.1371/journal.pntd.0004524>.
- Shi, P.-Y., Yin, Z., Nilar, S., Keller, T.H., 2011. *Dengue drug discovery*. In: Richard, L., Elliott, R.L. (Eds.), *Third World Diseases - Topics in Medicinal Chemistry*, 7, pp. 243–276.
- Schuler-Faccini, L., Ribeiro, E.M., Feitosa, I.M.L., Horovitz, D.D.G., Cavalcanti, D.P., Pessoa, A., Doriqui, M.J.R., Neri, J.I., de Pina Neto, J.M., Wanderley, H.Y.C., Cernach, M., El-Husny, A.S., Pone, M.V.S., Seroa, C.L.C., Sanseverino, M.T.V., Force, B.M.G.S.E.T., 2016. Possible association between zika virus infection and microcephaly — Brazil, 2015. *Morb. Mortal. Wkly. Rep.* 65, 59–62. <https://doi.org/10.2307/24856988>.
- Shiryayev, S.A., Farhy, C., Pinto, A., Huang, C.-T., Simonetti, N., Ngono, A.E., Dewing, A., Shrestha, S., Pinkerton, A.B., Cieplak, P., Strongin, A.Y., Terskikh, A.V., 2017. Characterization of the Zika virus two-component NS2B-NS3 protease and structure-assisted identification of allosteric small-molecule antagonists. *Antivir. Res.* 143, 218–229. <https://doi.org/10.1016/j.antiviral.2017.04.015>.
- Simonin, Y., Erkilic, N., Damodar, K., Clé, M., Desmetz, C., Bolloré, K., Taleb, M., Torriano, S., Barthelemy, J., Dubois, G., Lajoix, A.D., Foulongne, V., Tuailon, E., Van de Perre, P., Kalatzis, V., Salinas, S., 2019. Zika virus induces strong inflammatory responses and impairs homeostasis and function of the human retinal pigment epithelium. *EBioMedicine* 39, 315–331. <https://doi.org/10.1016/j.ebiom.2018.12.010>.
- Somnuk, P., Hauhart, R.E., Atkinson, J.P., Diamond, M.S., Avirutnan, P., 2011. N-linked glycosylation of dengue virus NS1 protein modulates secretion, cell-surface expression, hexamer stability, and interactions with human complement. *Virology* 413, 253–264. <https://doi.org/10.1016/j.virol.2011.02.022>.
- Souza, I.N. de O., Frost, P.S., França, J.V., Nascimento-Viana, J.B., Neris, R.L.S., Freitas, L., Pinheiro, D.J.L.L., Nogueira, C.O., Neves, G., Chimelli, L., Felice, F.G.D., Cavaleiro, É.A., Ferreira, S.T., Assunção-Miranda, I., Figueiredo, C.P., Poian, A.T. D., Clarke, J.R., 2018. Acute and chronic neurological consequences of early-life Zika virus infection in mice. *Sci. Transl. Med.* 10 <https://doi.org/10.1126/scitranslmed.aar2749>.
- Stefanik, M., Formanova, P., Bily, T., Vancova, M., Eyer, L., Palus, M., Salat, J., Braconi, C.T., Zanotto, P.M. de A., Gould, E.A., Ruzek, D., 2018. Characterisation of Zika virus infection in primary human astrocytes. *BMC Neurosci.* 19, 5. <https://doi.org/10.1186/s12868-018-0407-2>.
- Steinbach, R.J., Haese, N.N., Smith, J.L., Colgin, L.M.A., MacAllister, R.P., Greene, J.M., Parkins, C.J., Kempton, J.B., Porsov, E., Wang, X., Renner, L.M., McGill, T.J., Dozier, B.L., Kreklywich, C.N., Andoh, T.F., Grafe, M.R., Pecoraro, H.L., Hodge, T., Friedman, R.M., Houser, L.A., Morgan, T.K., Stenzel, P., Lindner, J.R., Schelonka, R. L., Sacha, J.B., Roberts, V.H.J., Neuringer, M., Brigande, J.V., Kroenke, C.D., Frias, A.E., Lewis, A.D., Kelleher, M.A., Hirsch, A.J., Streblow, D.N., 2020. A neonatal nonhuman primate model of gestational Zika virus infection with evidence of microcephaly, seizures and cardiomyopathy. *PLoS One* 15, e0227676. <https://doi.org/10.1371/journal.pone.0227676>.
- Sung, C., Wei, Y., Watanabe, S., Lee, H.S., Khoo, Y.M., Fan, L., Rathore, A.P.S., Chan, K. W.-K., Choy, M.M., Kamaraj, U.S., Sessions, O.M., Aw, P., de Sessions, P.F., Lee, B., Connolly, J.E., Hibberd, M.L., Vijaykrishna, D., Wijaya, L., Ooi, E.E., Low, J.G.-H., Vasudevan, S.G., 2016. Extended evaluation of virological, immunological and pharmacokinetic endpoints of CELADEN: a randomized, placebo-controlled trial of celgovisvir in dengue fever patients. *PLoS Neglected Trop. Dis.* 10 <https://doi.org/10.1371/journal.pntd.0004851>.
- Sunkara, P.S., Kang, M.S., Bowlin, T.L., Liu, P.S., Tyms, A.S., Sjoerdsma, A., 1990. Inhibition of glycoprotein processing and HIV replication by castanospermine analogues. *Ann. N. Y. Acad. Sci.* 616, 90–96. <https://doi.org/10.1111/j.1749-6632.1990.tb17831.x>.
- Taylor, D.L., Kang, M.S., Brennan, T.M., Bridges, C.G., Sunkara, P.S., Tyms, A.S., 1994. Inhibition of alpha-glucosidase I of the glycoprotein-processing enzymes by 6-O-butanoyl castanospermine (MDL 28,574) and its consequences in human immunodeficiency virus-infected T cells. *Antimicrob. Agents Chemother.* 38, 1780–1787. <https://doi.org/10.1128/AAC.38.8.1780>.
- Tsai, T.-T., Chen, C.-L., Lin, Y.-S., Chang, C.-P., Tsai, C.-C., Cheng, Y.-L., Huang, C.-C., Ho, C.-J., Lee, Y.-C., Lin, L.-T., Jhan, M.-K., Lin, C.-F., 2016. Microglia retard dengue virus-induced acute viral encephalitis. *Sci. Rep.* 6, 27670. <https://doi.org/10.1038/srep27670>.
- Vieira, M.A. da C. e S., Castro, A.A. de S., Henriques, D.F., Silva, E.V.P. da, Tavares, F.N., Martins, L.C., Guimarães, L.M., Monteiro, T.A.F., Azevedo, R. do S. da S., Cruz, A.C. R., Vasconcelos, P.F. da C., Vieira, M.A. da C. e S., Castro, A.A. de S., Henriques, D.F., Silva, E.V.P. da, Tavares, F.N., Martins, L.C., Guimarães, L.M., Monteiro, T.A.F., Azevedo, R. do S. da S., Cruz, A.C.R., Vasconcelos, P.F. da C., 2018. Encephalitis associated with Zika virus infection and reactivation of the varicella-zoster virus in a Brazilian child. *Rev. Soc. Bras. Med. Trop.* 51, 390–392. <https://doi.org/10.1590/0037-8682-0447-2017>.
- Walker, B.D., Kowalski, M., Goh, W.C., Kozarsky, K., Krieger, M., Rosen, C., Rohrschneider, L., Haseltine, W.A., Sodroski, J., 1987. Inhibition of human immunodeficiency virus syncytium formation and virus replication by castanospermine. *Proc. Natl. Acad. Sci. Unit. States Am.* 84, 8120–8124. <https://doi.org/10.1073/pnas.84.22.8120>.
- Walter, S., Fassbender, K., Gulbins, E., Liu, Y., Rieschel, M., Herten, M., Bertsch, T., Engelhardt, B., 2002. Glycosylation processing inhibition by castanospermine prevents experimental autoimmune encephalomyelitis by interference with IL-2 receptor signal transduction. *J. Neuroimmunol.* 132, 1–10. [https://doi.org/10.1016/S0165-5728\(02\)00308-9](https://doi.org/10.1016/S0165-5728(02)00308-9).
- Warfield, K.L., Warren, T.K., Qiu, X., Wells, J., Mire, C.E., Geisbert, J.B., Stuthman, K.S., Garza, N.L., Van Tongeren, S.A., Shurtleff, A.C., Agans, K.N., Wong, G., Callahan, M. V., Geisbert, T.W., Klöse, B., Ramstedt, U., Treston, A.M., 2017. Assessment of the potential for host-targeted iminosugars UV-4 and UV-5 activity against filovirus infections in vitro and in vivo. *Antivir. Res.* 138, 22–31. <https://doi.org/10.1016/j.antiviral.2016.11.019>.
- Watanabe, S., Rathore, A.P.S., Sung, C., Lu, F., Khoo, Y.M., Connolly, J., Low, J., Ooi, E. E., Lee, H.S., Vasudevan, S.G., 2012. Dose- and schedule-dependent protective efficacy of celgovisvir in a lethal mouse model for dengue virus infection informs dosing regimen for a proof of concept clinical trial. *Antivir. Res.* 96, 32–35. <https://doi.org/10.1016/j.antiviral.2012.07.008>.
- Whitby, K., Pierson, T.C., Geiss, B., Lane, K., Engle, M., Zhou, Y., Doms, R.W., Diamond, M.S., 2005. Castanospermine, a potent inhibitor of dengue virus infection in vitro and in vivo. *J. Virol.* 79, 8698–8706. <https://doi.org/10.1128/JVI.79.14.8698-8706.2005>.
- Whitby, K., Taylor, D., Patel, D., Ahmed, P., Tyms, A.S., 2004. Action of celgovisvir (6 O-butanoyl castanospermine) against the pestivirus BVDV: implications for the treatment of hepatitis C. *Antivir. Chem. Chemother.* 15, 141–151. <https://doi.org/10.1177/095632020401500304>.
- Willenborg, D.O., Parish, C.R., Cowden, W.B., 1992. Inhibition of adjuvant arthritis in the rat by phosphosugars and the  $\alpha$ -glucosidase inhibitor castanospermine. *Immunol. Cell Biol.* 70, 369–377. <https://doi.org/10.1038/icb.1992.49>.
- Willenborg, D.O., Parish, C.R., Cowden, W.B., 1989. Inhibition of experimental allergic encephalomyelitis by the  $\alpha$ -glucosidase inhibitor castanospermine. *J. Neurol. Sci.* 90, 77–85. [https://doi.org/10.1016/0022-510X\(89\)90047-6](https://doi.org/10.1016/0022-510X(89)90047-6).
- Winkler, G., Randolph, V.B., Cleaves, G.R., Ryan, T.E., Stollar, V., 1988. Evidence that the mature form of the flavivirus nonstructural protein NS1 is a dimer. *Virology* 162, 187–196. [https://doi.org/10.1016/0042-6822\(88\)90408-4](https://doi.org/10.1016/0042-6822(88)90408-4).
- Wong, M.-L., Rettori, V., Al-Shekhlee, A., Bongiorno, P.B., Canteros, G., McCann, S.M., Gold, P.W., Licinio, J., 1996. Inducible nitric oxide synthase gene expression in the brain during systemic inflammation. *Nat. Med.* 2, 581–584. <https://doi.org/10.1038/nm0596-581>.
- Yang, S., Xu, M., Lee, E.M., Gorshkov, K., Shiryayev, S.A., He, S., Sun, W., Cheng, Y.-S., Hu, X., Tharappel, A.M., Lu, B., Pinto, A., Farhy, C., Huang, C.-T., Zhang, Z., Zhu, W., Wu, Y., Zhou, Y., Song, G., Zhu, H., Shamim, K., Martínez-Romero, C., García-Sastre, A., Preston, R.A., Jayaweera, D.T., Huang, R., Huang, W., Xia, M., Simeonov, A., Ming, G., Qiu, X., Terskikh, A.V., Tang, H., Song, H., Zheng, W., 2018. Emetine inhibits Zika and Ebola virus infections through two molecular mechanisms: inhibiting viral replication and decreasing viral entry. *Cell Discov* 4, 1–14. <https://doi.org/10.1038/s41421-018-0034-1>.
- Zukor, K., Wang, H., Siddharthan, V., Julander, J.G., Morrey, J.D., 2018. Zika virus-induced acute myelitis and motor deficits in adult interferon  $\alpha\beta/\gamma$  receptor knockout mice. *J. Neurovirol.* 24, 273–290. <https://doi.org/10.1007/s13365-017-0595-z>.